



Tipping Points in the Mangrove March: Characterization of Biogeochemical Cycling Along the Mangrove–Salt Marsh Ecotone

Havalend E. Steinmuller,¹ Tammy E. Foster,² Paul Boudreau,¹ C. Ross Hinkle,¹ and Lisa G. Chambers^{1*} 

¹Department of Biology, University of Central Florida, 4000 Central Florida Blvd., Orlando, Florida 32816, USA; ²Kennedy Space Center Ecological Program, IMSS-300, Kennedy Space Center, Brevard County, Florida 32899, USA

ABSTRACT

Coastal wetland vegetation communities can respond to sea level rise via the encroachment of more salt- and inundation-tolerant species into existing vegetation communities. Black mangroves (*Avicennia germinans* L.) are encroaching on saltgrass (*Distichlis spicata* L.) within the Merritt Island National Wildlife Refuge in east central Florida (USA). Nine soil cores collected along three transects captured the transitions of both perceived abiotic drivers (salinity and inundation) and vegetation communities during both high- and low-water seasons to investigate patterns in soil biogeochemical cycling of carbon (C), nitrogen (N), and phosphorus (P). Results showed no change in soil carbon dioxide production along the ecotone during either season, though changes in enzyme activity and mineralization rates of N and P could indicate changes in C quality and nutrient availability affecting C degradation along the ecotone.

All parameters, excluding microbial biomass carbon, showed higher rates of activity or availability during the low-water season. Long-term soil nutrient stores (total C, N, P) were greatest in the saltgrass soils and similar between the mangrove and transition zone soils, indicating a ‘tipping point’ in biogeochemical function where the transition zone is functionally equivalent to the encroaching mangrove zone. Indicators of current biogeochemical cycling (that is, enzyme activity, potentially mineralizable N rates, and extractable ammonium concentrations) showed alterations in activity across the ecotone, with the transition zone often functioning with lower activity than within end members. These indicators of current biogeochemical cycling change in advance of full vegetation shifts. Increases in salinity and inundation were linked to mangrove encroachment.

Key words: mangrove encroachment; decomposition; nutrient availability; coastal wetlands; blue carbon; biogeochemical cycling; sea level rise.

Received 4 February 2019; accepted 3 June 2019

Electronic supplementary material: The online version of this article (<https://doi.org/10.1007/s10021-019-00411-8>) contains supplementary material, which is available to authorized users.

Author's Contribution HES, TEF, CRH, and LGC conceived and designed the study. H. Steinmuller performed research, analyzed data, and wrote the paper. PB performed research. All authors contributed to editing the manuscript.

*Corresponding author; e-mail: Lisa.Chambers@ucf.edu

HIGHLIGHTS

- Tipping point of soil biogeochemical change: transition zone functions similarly to mangrove.
- Biogeochemical indicators change in advance of full mangrove conversion.
- Salinity and inundation gradients co-occur with vegetation change.
- Higher total carbon in soils dominated by salt-grass, rather than mangroves.

INTRODUCTION

Globally, coastal wetlands can respond to relative rates of sea level rise in one of three ways: vertical accretion to ‘keep pace’ with sea level, landward transgression, or wetland submergence (Kirwan and Megonigal 2013). Landward transgression occurs when a minimally disturbed coastal wetland experiences a gradual rate of relative sea level rise that exceeds the rate of accretion. Changing abiotic factors disrupt the classic zonation of vegetation within salt marsh ecosystems, pressuring vegetation to slowly migrate upslope to continually occupy their optimal ecological niche (Bertness 1991; Donnelly and Bertness 2001; Morris and others 2002). Also known as ‘coastal squeeze’, landward transgression is occurring around the globe, resulting in ecosystem conversion when wetlands begin to converge upon immovable, developed upland systems (Pontee 2013; Torio and Chmura 2013).

In addition to vegetation communities changing position within the coastal plain, the altered physicochemical environment as a result of sea level rise can catalyze the encroachment of more salt- and flood-tolerant species along the seaward edge of coastal wetlands (that is, Donnelly and Bertness 2001; Rogers and others 2006). Although global poleward expansion of mangroves is attributed to latitudinal expansion from decreased frequency of extreme freeze events (Cavanaugh and others 2014), regional landward transgression is occurring where mangroves are able to opportunistically invade marshes by outcompeting the stressed native vegetation (Raabe and others 2012; Kelleway and others 2016). Within south and central Florida (USA), mangroves are expanding along the coastal fringe and altering coastal wetland function and structure (Saintilan and others 2014), as they are able to tolerate high salinities and wide fluctuations in water levels. For example, the salt marsh to mangrove conversion rate within

Tampa Bay (FL) wetlands is 72% over 125 years (Raabe and others 2012). Though mangroves are able to stabilize shorelines, provide buffer from storm surge, trap tidal debris and sediments, and provide shade and habitat, knowledge gaps still exist in understanding the full extent of ecosystem consequences of mangrove encroachment on native salt marshes (Field and others 1998; Kelleway and others 2017).

Perhaps, the most well-documented ecological consequence occurring with mangrove encroachment into salt marshes concerns ecosystem C stocks. Mangroves are structurally and physiologically distinct from salt marsh grasses, which contributes to differences in potential C storage within biomass (Duarte and others 2013). Multiple studies have reported greater potentials for C storage within both the aboveground and belowground compartments of mangroves relative to salt marsh grasses (Duarte and others 2013; Doughty and others 2016; Kelleway and others 2016). However, in addition to aboveground and belowground C storage within plant parts, there have been documented differences in the mangrove and salt marsh C deposition and burial (Lunstrum and Chen 2014; Doughty and others 2016). Although C accumulation is a critical factor in understanding C dynamics between the two vegetation types, the residence time and quality (that is, chemical structure) of C could affect long-term C storage. Mangroves generally contain more recalcitrant compounds that require more energy to decompose than their salt marsh grass counterparts (Bianchi and others 2013; Middleton and Mckee 2014). To date, very few studies have focused on differences in soil respiration between the two vegetation types, which factors heavily into source–sink dynamics of C within coastal wetlands experiencing mangrove encroachment (Barreto and others 2018; Lewis and others 2014; Simpson and others 2019).

The breakdown of organic matter also alters nutrient availability within coastal wetland soils. Thus, changes in soil respiration, soil quality, and vegetation type could alter the cycling of other biologically important macronutrients (nitrogen, phosphorus, and sulfur). Although many studies have focused on nutrient limitation (that is, total soil nutrients) within salt marsh and mangrove soils separately (Feller 1995; Feller and others 1999, 2003, 2013; Henry and Twilley 2013; Simpson and others 2013), no study has directly explored changes to biogeochemical cycling of nutrients as a result from encroachment. To understand mangrove encroachment and ecosys-

tem conversion as a whole, it is critical to examine the biogeochemical changes occurring within soils underlying these two vegetation types. The goal of this study is to fill this knowledge gap and evaluate microbially mediated biogeochemical cycling of C, nitrogen (N), and phosphorus (P) (that is, decomposition and nutrient availability) along a transect of mangrove encroachment into salt marsh during both the high- and low-water seasons in central Florida (USA). By implementing a space-for-time experimental design, we sought to determine the timescale (before, after, or concurrently with species shifts) upon which biogeochemical cycling is affected during mangrove encroachment by comparing biogeochemical functions in the transition zone to that of the two end-member community types. Furthermore, we anticipated the effects of encroachment may differ by season, such that the low-water season would increase decomposition and nutrient availability, whereas high-water season would dampen the magnitude of these measurements (Foster and others 2017), with varying ecosystem-level implications. To study the biogeochemical effects of mangrove encroachment, we constructed multiple competing hypotheses: (a) the null hypothesis, where vegetation community had no effect (Figure 1, panel A); (b) a linear trend in microbial activity and nutrient availability from one vegetation community to another, across the transition zone (Figure 1, panels B, E); (c) greatest microbial activity and nutrient availability within the end-member communities (Figure 1, panel C); (d) greatest microbial activity and nutrient availability within the transition zone (Figure 1, panel D); and (e) a tipping point in microbial activity and nutrient availability, where the transition zone is functionally the same as one end-member vegetation community (Figure 1, panels F, G). In addition to the effects of vegetation community on biogeochemical processes, we further hypothesized that a gradient of salinity and inundation would be present within the selected site; increases in both of these abiotic factors have been theorized to encourage mangrove encroachment into salt marshes (that is, Krauss and others 2011), but there remains a lack of empirical evidence linking the abiotic forcings to biotic gradients.

METHODS

Site Description

A site was selected to span the ecotone of encroachment of black mangrove (*Avicennia germinans*) on dominant endemic saltgrass (*Distichlis spi-*

cata L.) within the Merritt Island National Wildlife Refuge, Cape Canaveral, FL (Figure 2). Henceforth, the salt marsh plot will be referred to by the common name of the dominant species, saltgrass, and the black mangrove plot will be referred to simply as ‘mangrove.’ Specifically, the site was located within the cell designated as T9-North by the Brevard County Mosquito Control (28°42′49.71″N, 80°44′32.99″W). Soils at the site are fine, smectitic, nonacid hyperthermic typic hydraquent soils (Turnbull muck and Riomar clay loam). Mangroves at the site were defined as dwarf or fringe mangroves as exist within the warm temperate zone and exhibit shorter tree heights when compared to mangroves within subtropical zones (Doughty and others 2016). Within a proximal site, Simpson and others (2017) recorded canopy heights as 0.84 ± 0.1 m. Mangrove encroachment within this site was characterized by Doughty and others (2016), who found that mangrove aerial extent increased 69% within a seven-year period. Three transects consisting of three plots (4 m²) were established to span the ecotone, with end members in both the mangrove and saltgrass and one plot within the transition zone, where both mangroves and saltgrass are present. The site experienced peak precipitation between June to September; combined with seasonal variation of water levels within the adjacent estuary (Indian River Lagoon, IRL) through a seasonal seiche, the high-water season occurred during August–November (Figure 3), while low-water season occurred during February–April (Brockmeyer and others 2005).

Soil Sampling

Soil sampling was conducted within two separate seasons that will be henceforth referred to as high water (August 2017) and low water (February 2018). Sampling consisted of obtaining three cores per plot (for a total of 27 cores per site per season) down to 30 cm via the push-core method. Cores were field-extruded into three 10-cm intervals: 0–10, 10–20, and 20–30 cm. Samples were immediately transferred into gallon-sized polyethylene bags and transported back to the laboratory where they were stored at 4°C until sample analysis was completed.

Salinity and Elevation Data

Surface water salinity was determined at each plot along the middle transect during both the high- and low-water sampling by use of a handheld optical refractometer (ThermoFisher Scientific, Waltham, MA). Elevation was determined by use

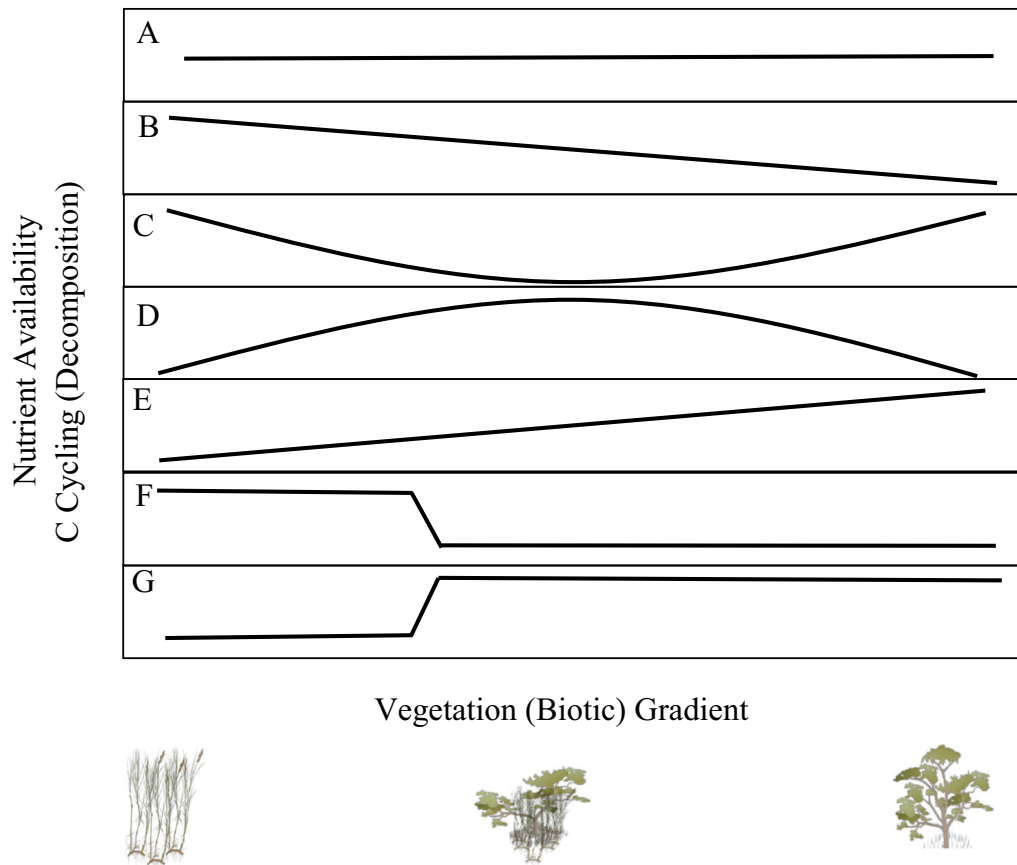


Figure 1. Conceptual diagram outlining hypotheses where (A) is the null hypothesis (no change), (B) represents higher microbial activity and nutrient availability in the first vegetation community type coinciding with low salinity and inundation, (C) represents higher microbial activity and nutrient availability within the end members (both high and low inundation and salinity), (D) represents higher microbial activity and nutrient availability within the transition zone (moderate inundation and salinity), and (E) represents higher microbial activity and nutrient availability within the second vegetation community type (high inundation and salinity).

of a Trimble Geo 7x (Trimble Inc., Sunnyvale, California, USA) coupled with LiDAR data (NAVD88).

Soil Physicochemical Parameters

Soil moisture content was determined by drying a subsample of soil within a gravimetric oven for 3 days at 70°C, when a constant weight was achieved. Bulk density was calculated based on soil wet weight and volume for all samplings at all sites except for high water within the mangrove site. Following drying, soils were ground using a SPEX Sample Prep 8000 M Mixer Mill (Metuchen, NJ). The loss-on-ignition method was used to determine percent organic matter within the dried, ground subsamples. Following determination of percent organic matter via ashing at 550°C in a muffle furnace for a total of 3 h, soils were digested with 50 mL of 1 M HCl at 100°C for 30 min and then

filtered through Whatman #41 filters for total P analysis (Andersen, 1976 with modifications). Total P content was measured colorimetrically on an AQ2 Automated Discrete Analyzer (Seal Analytical, Mequon, WI) via EPA method 365.1 (Rev.2). Total C and total N were determined on dried, ground subsamples on a Vario Micro Cube CHNS Analyzer (Elementar Americas Inc., Mount Laurel, NJ). Soil pH was determined by creating a 1:5 slurry of soil to distilled, deionized water and measured using an Accumet benchtop pH probe (AccumetXL200, ThermoFisher Scientific, Waltham, MA, USA).

Extractable Nutrients and Microbial Biomass

Extractable nutrient analyses [nitrate (NO_3^-), ammonium (NH_4^+), soluble reactive phosphorus (SRP)] were conducted immediately upon return to the laboratory. Approximately 2.5 g of field-moist

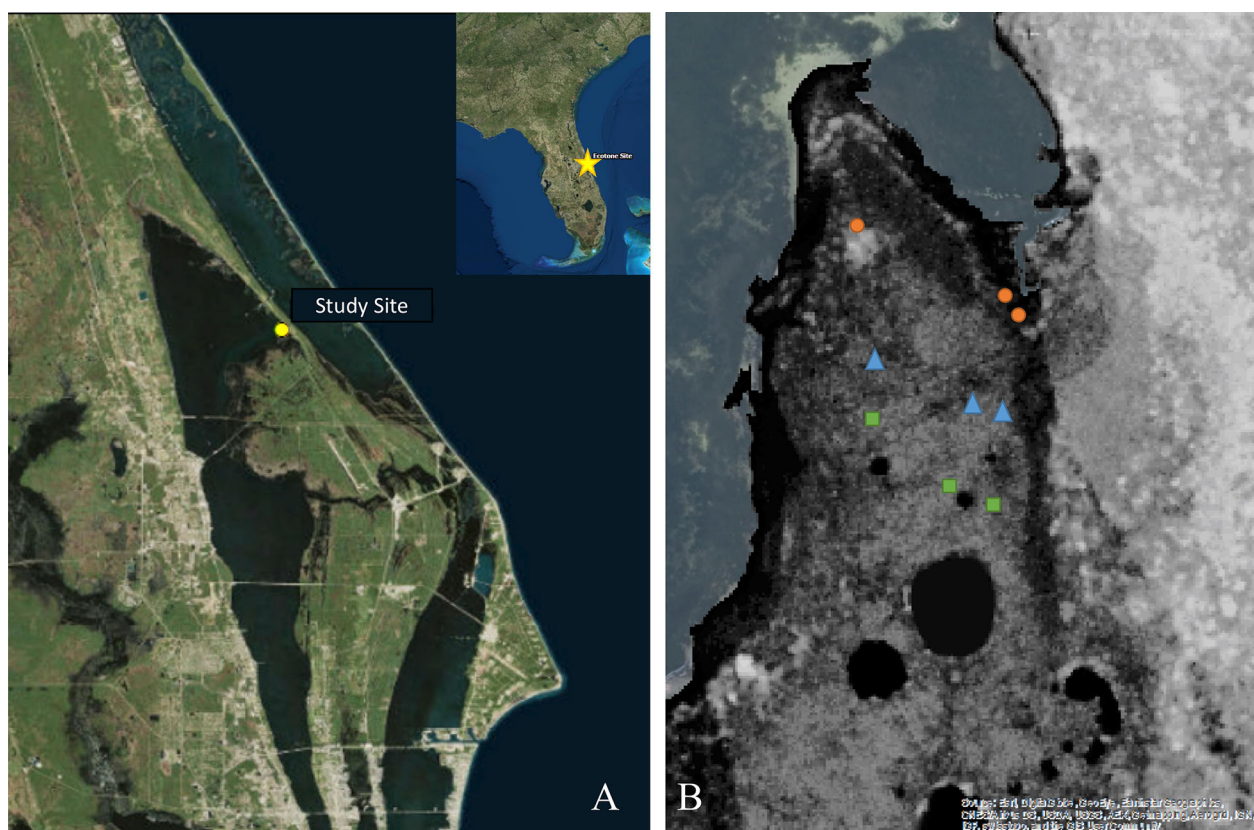


Figure 2. Map of the site, located within the Merritt Island National Wildlife Refuge (cell T9, $28^{\circ}42'49.71''\text{N}$, $80^{\circ}44'32.99''\text{W}$). (A) The site in the larger context of Eastern Florida, (B) digital elevation model depicting elevation at the site from LiDAR data (darker colors correspond to lower elevations) overlaid on aerial photography. Circles correspond to mangrove points, triangles indicate transition zone points, and squares indicate saltgrass points.

soils was weighed into 40-mL centrifuge tubes containing 25 mL of 2 M KCl. Samples were shaken at 125 rpm for 1 h and then centrifuged at 5000 rpm for 10 min at 10°C . Samples were filtered through Supor 0.45- μm filters and acidified with double-distilled (DD) H_2SO_4 to a pH of less than 2 for preservation. Samples were then analyzed colorimetrically on an AQ2 Automated Discrete Analyzer (Seal Analytical, Mequon, WI) within 28 days, according to EPA methods 231-A (Rev. 0), 210-A (Rev. 1), and 204-A (Rev. 0).

Similarly, replicate samples of 2.5 g field-moist soil were weighed into 40-mL centrifuge tubes and fumigated with chloroform for 24 h in a glass desiccator (Vance and others 1987). Following the fumigation, samples were extracted as outlined above. Both initial and fumigated samples were analyzed for dissolved organic carbon on a Shimadzu TOC-L Analyzer (Shimadzu Instruments, Kyoto, Japan). Microbial biomass C was calculated as the difference in dissolved organic carbon (DOC)

between the fumigated samples and non-fumigated samples.

Potential Greenhouse Gas Production

Following Bridgman and Ye 2013, samples were immediately homogenized upon return to the laboratory, and 7–10 g of soil from each sample was weighed into a 120-mL glass serum bottle. Bottles were capped with rubber septa, crimped with aluminum crimps, evacuated to -75 mmHg , and then purged with 99% O_2 -free N_2 gas for three minutes. Bottles were then injected with artificial seawater matching the surface water salinity at the time of sampling to create a 1:2 slurry of soil to artificial seawater. Bottles were placed on an orbital shaker in the dark at 100 rpm and 25°C . Samples of the headspace were taken at 24, 72, 120, 168, and 240 h and injected into a GC-2014 gas chromatograph (Shimadzu Instruments, Kyoto, Japan). Respiration rates were calculated as the change in CO_2 and methane production over time using

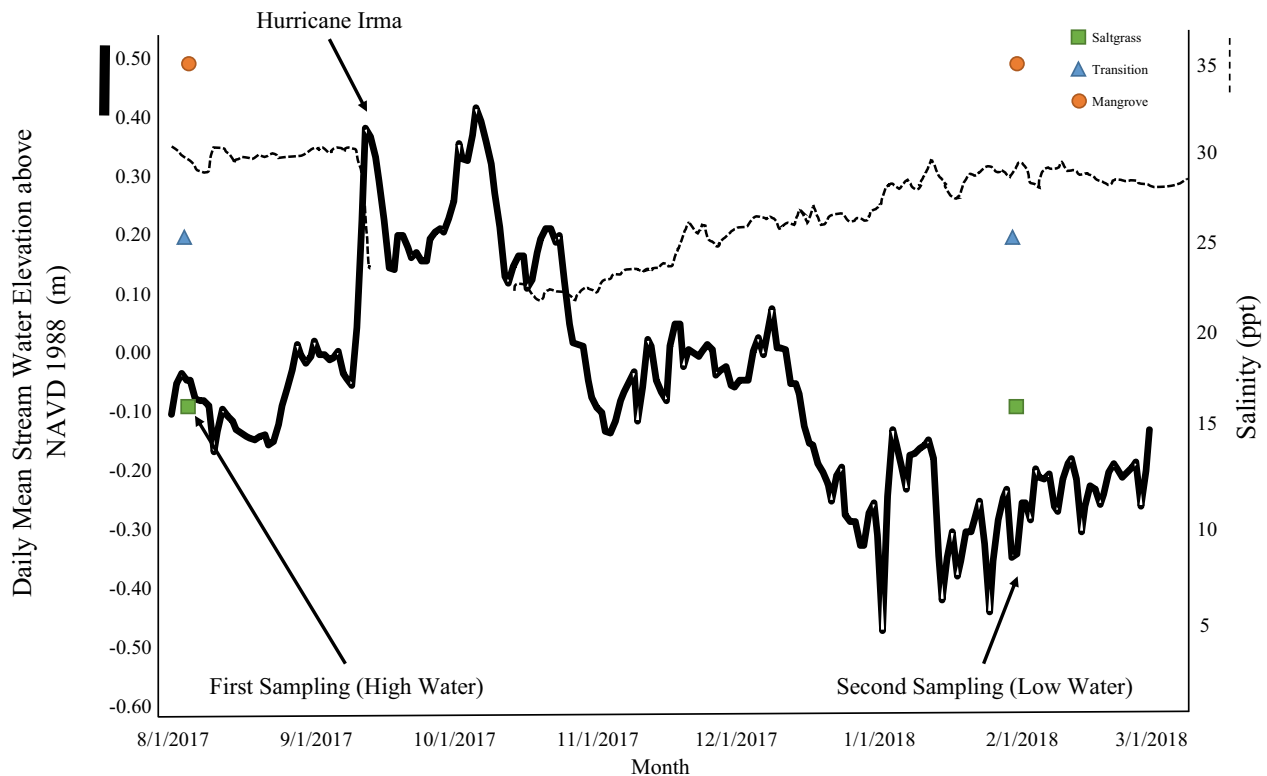


Figure 3. Daily mean stream water elevation (solid black line) above NAVD 1988 (m) at Haulover Canal, Mims, FL (< 1.1 km from site, data from USGS station 02248380), and ambient salinity (dashed black line) of the Indian River Lagoon at Max Brewer Memorial Parkway Fishing Pier (SJRWMD 33954622-CM, 10 km from site) from 8/01/2017 to 3/01/2017. Symbols indicate ambient salinity at each plot during sampling (circles = mangrove, triangles = transition, squares = saltgrass).

Henry's law to determine the amount of CO_2 and CH_4 dissolved in either the liquid phase or within the headspace. Methane peak areas were consistently low (often below detection) and thus will not be discussed.

Potentially Mineralizable Nitrogen and Phosphorus

Following the 10-day bottle incubation outlined above, 25 mL of 2 M KCl was added to the bottles, which were then shaken for 1 h at 125 rpm and 25°C. Bottles were deconstructed, transferred to centrifuge tubes, and centrifuged for 10 min at 10°C. The supernatant was decanted, filtered using Supor 0.45- μm filters, and then acidified with DD H_2SO_4 to a pH of less than 2 for preservation. Samples were analyzed on an AQ2 Automated Discrete Analyzer (Seal Analytical, Mequon, WI) within 28 days. Rate of mineralization of N or P was calculated as the NH_4^+ (or SRP) concentration at day 10 minus the initial extractable NH_4^+ (or SRP) concentration, divided by 10 days.

Extracellular Enzyme Activity

Fluorometric assays were performed to determine activity of N-acetyl- β -D-glucosidase (NAG), alkaline phosphatase (AP), β -glucosidase (BG), xylosidase (XY), cellobiosidase (CB), and arylsulfatase (AS). Thirty-nine (39) mL of distilled, deionized water was added to approximately 0.5 g of field-moist soil and shaken for 1 h at 25°C and 125 rpm. Both samples and fluorescently labeled MUF-specific substrates for each enzyme were pipetted into clear 96-well plates and then measured on a BioTek synergy HTX (BioTek Instruments, Inc., Winooski, VT, USA) at excitation/emission wavelengths 360/460 nm. Samples were measured again 24 h later to determine a rate of enzyme activity.

Porewater Nutrients

During each sampling, porewater equilibrators (peepers) were deployed at each plot to determine porewater nutrient (NH_4^+ , NO_3^- , SRP, DOC) concentrations and specific conductivity with depth. Prior to deployment, peepers were filled with N_2 -

purged nanopure water and then assembled and transported within an anaerobic environment. Peepers were left to equilibrate within the soil for 10 days. Immediately after removal from the soil, sample wells were extracted using a syringe and consolidated into seven separate 5-cm increments down to 35 cm. Samples were filtered using 0.45- μm syringe filters and acidified with DD H_2SO_4 to a pH of less than 2. Samples were placed on ice for transportation back to the laboratory. Ammonium, NO_3^- , and SRP concentrations were determined colorimetrically on an AQ2 Automated Discrete Analyzer (Seal Analytical, Mequon, WI) within 28 days. Porewater NO_3^- concentrations were consistently below detection limits and thus will not be discussed. Dissolved organic carbon concentrations were analyzed via a Shimadzu TOC-L Analyzer (Shimadzu Instruments, Kyoto, Japan). Specific conductivity was determined by use of an Accumet bench top conductivity probe (Accumet XL200, ThermoFisher Scientific, Waltham, MA).

Statistical Analysis

Data were separated by season for statistical analyses because parameters tended to vary significantly between high- and low-water seasons; our interest was in understanding the effects of vegetation community on biogeochemistry under these two distinct abiotic conditions. Data analysis was performed in R (R Foundation for Statistical Computing, Vienna, Austria) via RStudio (RStudio Inc., Boston, MA, USA). Before determining significance, each parameter was analyzed for assumptions of normality using the Shapiro–Wilk test and homogeneity of variance using Levine’s test. A log transform was applied to data from each parameter to meet these assumptions. Data were analyzed with a linear mixed model (package ‘lme4’, model—lme), accounting for soil depth and vegetation community as fixed effects, while the random effects included replicate core nested in transect. The interaction between depth and vegetation community was consistently non-significant and was thus removed from the model during the process of model simplification/selection and validation using AIC scores (Burnham and Anderson 2002; Akaike 1974, 1983; Bozdogan 1987). Due to the number of iterations of the model performed, a Bonferroni correction was applied to the alpha value of 0.1 to reduce the likelihood of Type I error, lowering the p value to reject the null hypothesis to 0.005 (Bonferroni 1936; Dunn 1961). Least-square means post hoc tests were used to determine differences among vegetation types and depth intervals.

RESULTS

Salinity and Elevation

The mangrove plots had the lowest elevation, averaging -9.15 ± 0.23 cm (NAVD88). Elevation within the transition zone plots averaged 0.069 ± 2.58 cm, and the saltgrass plots averaged 5.99 ± 2.16 cm. Elevation was used as a proxy for water level throughout the experiment with lower elevations corresponding to higher water level. During high water, salinity (as determined by refractometer) at the mangrove plots was highest, approximately 35 ppt, followed by the transition plots and saltgrass plots, which were approximately 25 and 15 ppt, respectively (Figure 3). Low-water prevented measurement of surface water salinity and the high-water salinity measurements were used for bottle incubations (Figure 3).

Soil Physicochemical Properties

Both vegetation community and soil depth were significant predictors of soil moisture content and pH during both high- and low-water seasons (Table 1). During both seasons, the trend was the same: The saltgrass plots had significantly higher soil moisture than the transition and mangrove plots (which did not differ from one another), while pH was higher in the mangrove plots and did not differ between the transition and saltgrass (Figure 4). The highest soil moisture was observed in the saltgrass plots during high water (mean \pm standard error; $72 \pm 1.1\%$) and the lowest in the mangrove plots during low water ($54 \pm 3.6\%$; Table 2), which was an effect of the lower soil bulk density in the saltgrass plots, relative to the mangrove plots, due to the higher organic matter content. Soil moisture content decreased with depth, while pH increased with depth (Table 2). In general, soil moisture content showed a strong positive correlation with nearly all other biogeochemical parameters of interest, while pH demonstrated a negative correlation with several key parameters (for example, extractable NO_3^- , extractable SRP, potentially mineralizable nitrogen (PMN) rates, CO_2 production, and all enzyme activity), particularly during low-water season (Supplementary Table).

Total soil nutrient concentrations (C, N, P, and organic matter content) remained consistent between high- and low-water samplings and were affected by vegetation community and soil depth (Table 1). The saltgrass plots had the highest concentrations of every nutrient (Table 2), while the transition and the mangrove plots did not differ

Table 1. *p* Values for Each Tested Parameter Using the Linear Model

	Woody–Herbaceous Transition			
	High water		Low water	
	Community	Depth	Community	Depth
Moisture content	<u>0.0001</u>	<u>0.0001</u>	<u>0.0007</u>	<u>0.0003</u>
Total C	<u>< 0.0001</u>	<u>< 0.0001</u>	<u>< 0.0001</u>	<u>< 0.0001</u>
Total N	<u>< 0.0001</u>	<u>< 0.0001</u>	<u>< 0.0001</u>	<u>< 0.0001</u>
Total P	<u>0.0001</u>	<u>< 0.0001</u>	<u>0.0040</u>	<u>< 0.0001</u>
Organic matter	<u>< 0.0001</u>	<u>< 0.0001</u>	<u>< 0.0001</u>	<u>< 0.0001</u>
pH	<u>< 0.0001</u>	<u>0.0002</u>	<u>< 0.0001</u>	<u>< 0.0001</u>
Ext. nitrate	0.1185	0.1583	<u>< 0.0001</u>	<u>< 0.0001</u>
Ext. ammonium	0.0370	0.6668	<u>0.0001</u>	0.0753
Ext. SRP	<u>0.0020</u>	<u>0.0005</u>	0.0121	<u>< 0.0001</u>
Microbial biomass C	0.0072	0.8358	<u>0.0001</u>	<u>< 0.0001</u>
NAG	0.0406	<u>0.0001</u>	0.0140	<u>< 0.0001</u>
AP	<u>0.0022</u>	<u>0.0002</u>	<u>< 0.0001</u>	<u>< 0.0001</u>
BG	<u>0.0008</u>	<u>< 0.0001</u>	0.0559	<u>< 0.0001</u>
CB	<u>0.0041</u>	<u>0.0002</u>	0.0299	<u>< 0.0001</u>
XY	<u>0.0003</u>	<u>0.0001</u>	<u>< 0.0001</u>	<u>< 0.0001</u>
AS	<u>0.0030</u>	<u>0.0010</u>	<u>0.0001</u>	<u>< 0.0001</u>
CO ₂ production	0.1874	<u>0.0002</u>	0.0756	<u>< 0.0001</u>
PMN	0.0088	0.0119	<u>0.0012</u>	<u>< 0.0001</u>
PMP	0.1123	<u>0.0009</u>	0.0091	<u>< 0.0001</u>

Fixed effects included community type and depth, and random effects included transect and replicate. The applied Bonferroni correction lowered the α value to 0.005. Underlined values are significant. ($n = 81$ for each season).

from one another (Figure 4). All concentrations decreased with increasing soil depth and showed strong positive correlations to all other biogeochemical parameters except extractable NH_4^+ (Table 2; Supplemental Table).

Extractable Nutrients and Potentially Mineralizable Nutrients

Neither depth nor vegetation community significantly predicted extractable NO_3^- or NH_4^+ concentrations during high water (Table 1, Figure 5). High-water extractable SRP differed between the saltgrass plots, averaging $2.11 \pm 0.295 \text{ mg kg}^{-1}$, and transition plots, $1.01 \pm 0.203 \text{ mg kg}^{-1}$ (Table 1, Figure 4). Extractable SRP during high water was significantly correlated with PMN and potentially mineralizable phosphorus (PMP) rates, CO₂ production, and all enzyme activity (Supplementary Table). High-water extractable NO_3^- was correlated with PMP rates, NAG activity, phosphatase activity, xylosidase activity, and sulfatase activity. In contrast, high-water extractable ammonium concentrations were correlated with extractable SRP concentrations, NAG activity, and sulfatase activity.

During low water, extractable NO_3^- and NH_4^+ were significantly different between vegetation communities, while extractable NO_3^- and SRP were significantly different between depths (Table 1). The highest extractable NO_3^- concentrations during low water were within the saltgrass plots, averaging $2.02 \pm 0.211 \text{ mg kg}^{-1}$; lowest concentrations were within the mangroves, averaging $1.36 \pm 0.128 \text{ mg kg}^{-1}$, but the transition and mangrove plots did not differ from one another (Figure 4). Low-water extractable NO_3^- concentrations were roughly 3.5 \times higher than concentrations during high water. Extractable NO_3^- concentrations were positively correlated with extractable NH_4^+ concentrations, extractable SRP concentrations, PMP and PMN rates, MBC, CO₂ production, and all enzyme activity (Supplementary Table). Extractable NH_4^+ concentrations during low water ranged from 18.1 ± 4.43 to $5.43 \pm 0.764 \text{ mg kg}^{-1}$ within the mangrove and transition plots, respectively (Figure 5). Concentrations within the saltgrass plots and transition plots did not differ during low water (Figure 4). Low-water extractable NH_4^+ was significantly correlated with PMP rates, MBC, and cellobiosidase activity (Supplementary Table), and concentrations







	High-Water			Low-Water		
						
	Mangrove	Transition	Saltgrass	Mangrove	Transition	Saltgrass
Moisture Content	-	-	●	-	-	●
Total C	-	-	●	-	-	●
Total N	-	-	●	-	-	●
Total P	-	-	●	-	●	-
Organic Matter	-	-	●	-	-	●
pH	●	-	-	●	-	-
Ext. Nitrate	-	-	-	●	●	●
Ext. Ammonium	-	-	-	●	-	-
Ext. SRP	-	-	-	-	-	-
Microbial Biomass C	-	-	-	-	-	●
NAG	-	-	-	-	-	-
AP	-	-	●	-	-	●
BG	-	●	-	-	-	-
CB	-	●	-	-	-	-
XY	-	-	●	-	-	●
AS	-	●	-	-	-	●
CO ₂ Production	-	-	-	-	-	-
PMN Rate	-	-	-	-	-	●
PMP Rate	-	-	-	-	-	-

Figure 4. Similarity matrix derived from post hoc least squares mean tests where the community effect was significant in the linear model. Dashes ('-') indicate no significant difference between vegetation communities (functionally the same), whereas black boxes indicate that a significant difference between vegetation communities.

were roughly $2.5\times$ higher than concentrations during high water. Low-water concentrations of extractable SRP were significantly correlated with PMN and PMP rates, MBC, CO₂ production, and all enzyme activity (Supplementary Table).

During high water, PMN rates were not significantly predicted by either community or depth (Table 1). During low water, both depth and vegetation significantly affected PMN rates (Table 1, Figure 5), which were roughly $2\times$ greater than during the high-water season. While the low-water transition plots were not different from the low-water mangrove plots, all other comparisons were significant (Figure 4). The low-water saltgrass plots contained the highest PMN rates, averaging $13.4 \pm 2.21 \text{ mg NH}_4^+ \text{ kg}^{-1} \text{ d}^{-1}$, whereas the mangrove and transition plots averaged $8.77 \pm 2.02 \text{ mg NH}_4^+ \text{ kg}^{-1} \text{ d}^{-1}$. High-water PMN rates were significantly correlated with PMP rates, CO₂ production, and all enzyme activity (Supplementary Table). Similarly, low-water PMN rates were significantly correlated with PMP rates, MBC, CO₂

production, and all enzyme activity (Supplementary Table).

Both high-water and low-water PMP rates were significantly influenced by depth (Table 1). High-water PMP rates were correlated with CO₂ production and all enzyme activity, while low-water PMP rates were correlated with MBC, CO₂ production, and all enzyme activity (Supplementary Table).

Microbial Biomass C and CO₂ Production

Microbial biomass C content was roughly $1.5\times$ higher during high water than during low water. Neither community type nor depth significantly predicted MBC content within the high-water season, and both significantly predicted MBC content during low water (Table 1, Figure 6). Microbial biomass C in the saltgrass plots at low water averaged $2303 \pm 312 \text{ mg kg}^{-1}$, which was significantly greater than both the transition and mangrove plots, which were not different from each other. The transition plots at low water contained

Table 2. Soil Physiochemical Properties by Season, Community, and Depth

Season	Community	Depth (cm)	pH		Moisture content (%)		Organic matter (%)		Total C (g kg ⁻¹)		Total N (g kg ⁻¹)		Total P (mg g ⁻¹)	
			Mean	StErr	Mean	StErr	Mean	StErr	Mean	StErr	Mean	StErr	Mean	StErr
High water	Saltgrass	0-10	5.45	0.10	76.08	0.64	64.90	1.61	312.39	7.51	20.34	0.49	502.69	21.66
		10-20	5.64	0.06	73.06	2.09	48.54	5.31	220.63	20.73	13.84	1.32	354.69	11.40
		20-30	6.19	0.06	69.00	2.30	43.32	4.14	208.61	20.31	12.89	1.24	297.80	10.35
	Transition	0-10	5.53	0.10	70.10	2.21	46.09	6.10	137.13	10.34	8.74	0.67	396.01	50.70
		10-20	5.90	0.08	61.65	5.94	30.81	6.87	118.39	25.64	7.61	1.65	241.80	40.40
		20-30	6.45	0.11	56.38	6.84	21.63	5.17	62.20	22.36	3.96	1.49	192.13	33.89
Low water	Mangrove	0-10	6.67	0.22	65.09	1.94	27.51	2.61	220.92	29.83	14.11	1.93	310.26	50.34
		10-20	6.60	0.26	57.34	4.00	26.47	5.60	158.50	37.42	9.57	2.21	265.30	58.02
		20-30	6.71	0.23	46.52	6.21	16.82	5.12	103.79	25.13	6.57	1.74	188.69	44.34
	Saltgrass	0-10	6.11	0.08	75.71	0.81	67.37	1.12	313.14	8.72	18.90	2.38	547.02	44.52
		10-20	6.48	0.07	71.66	1.99	46.88	5.74	210.55	26.87	13.75	1.77	321.24	41.06
		20-30	6.65	0.09	63.35	7.86	44.37	6.22	211.61	35.36	13.00	1.94	266.34	27.44
Transition	0-10	6.00	0.12	68.70	3.76	47.30	8.08	166.03	16.21	10.90	0.85	401.00	71.17	
	10-20	6.46	0.16	60.61	3.50	25.91	4.90	108.36	31.77	7.15	2.08	222.60	40.09	
	20-30	6.77	0.11	49.94	7.20	16.86	5.11	74.64	27.07	4.98	1.88	142.44	31.97	
Mangrove	0-10	6.53	0.23	62.39	6.71	37.16	3.26	224.21	34.63	15.14	2.27	439.65	43.68	
	10-20	6.78	0.20	56.23	4.68	23.86	5.99	109.33	20.81	7.38	1.44	259.30	53.27	
	20-30	7.00	0.16	44.64	6.40	16.21	5.28	78.31	23.95	5.29	1.67	190.34	44.72	

StErr stands for standard error (n = 9).

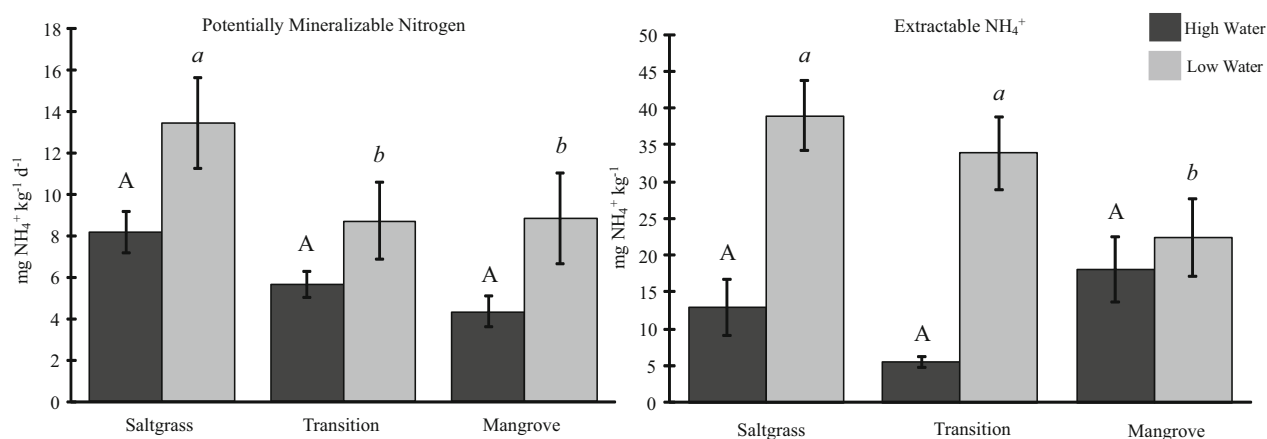


Figure 5. Potentially mineralizable N rates and extractable ammonium at high water and low water along transects of saltgrass, transition, and mangroves. Values are mean \pm standard error ($n = 9$). Dark bars represent high water levels, whereas light bars represent low water levels. Capital letters denote significance ($p < 0.05$) between high water means, whereas lowercase, italicized letters denote significance ($p < 0.05$) between low water means when the main effect was significant ($p < 0.005$).

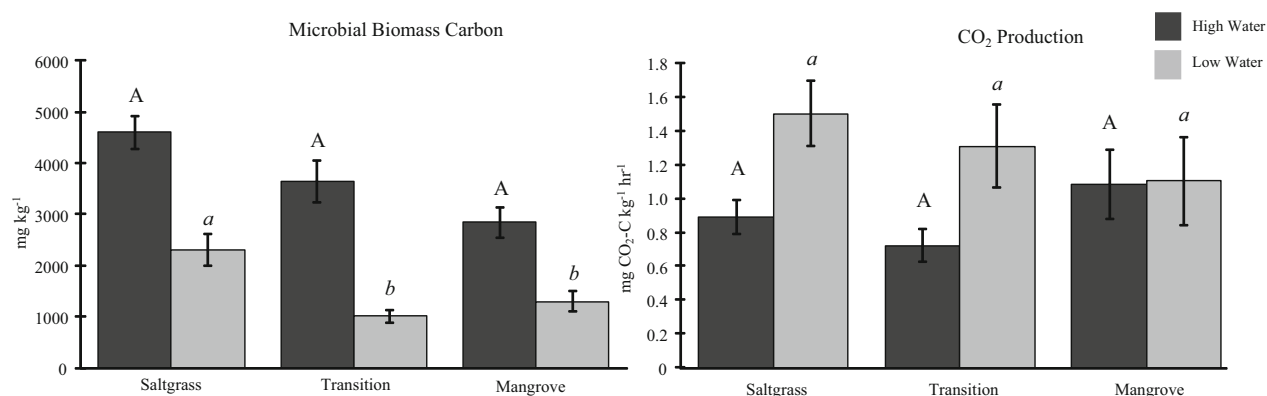


Figure 6. Microbial biomass C and rates of CO₂ production at high water and low water along transects of saltgrass, transition, and mangroves. Values are mean \pm standard error ($n = 9$). Dark bars represent high water levels, whereas light bars represent low water levels. Capital letters denote significance ($p < 0.05$) between high water means, whereas lowercase, italicized letters denote significance ($p < 0.05$) between low water means when the main effect was significant ($p < 0.005$).

an average MBC content of $1006 \pm 133 \text{ mg kg}^{-1}$. Low-water MBC was significantly correlated with PMN and PMP rates, CO₂ production, and all enzyme activity (Supplementary Table).

CO₂ production significantly differed with depth during both seasons, but not with vegetation community (Table 1, Figure 6). High-water CO₂ production rates were correlated with extractable SRP, PMN rates, PMP rates, and all enzyme activity. Carbon dioxide production was 30% higher during low water than during high water. Carbon dioxide production was positively correlated with all enzyme activity during low water (Supplementary Table).

Extracellular Enzyme Activity

Both BG and CB activities were significantly different between both vegetation community and depth during high water and only with depth during low water (Table 1, Figure 7). Activity of both BG and CB during low water was approximately 2.8 \times higher than activity during high water. Activity of BG at high water averaged $1.71 \pm 0.251 \text{ nmol MUF g}^{-1} \text{ h}^{-1}$ at the mangrove plots, which was not significantly different from activity at the saltgrass plots. The transition plots had the lowest activity at high water, averaging $1.02 \pm 0.161 \text{ nmol MUF g}^{-1} \text{ h}^{-1}$. Similarly, high-water CB activity ranged from $0.524 \pm 0.043 \text{ nmol}$

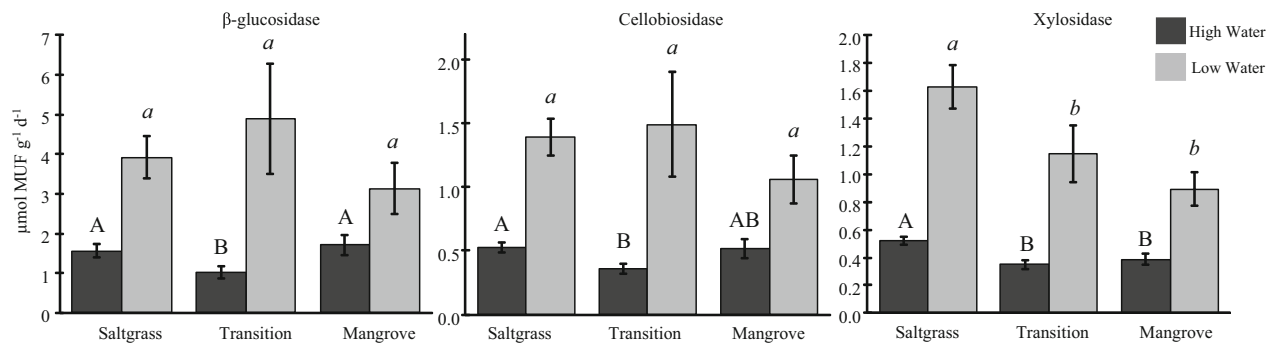


Figure 7. Enzyme activity of C enzymes (BG, CB, XY) at high water and low water along transects of saltgrass, transition, and mangroves. Values are mean \pm standard error ($n = 9$). Dark bars represent high water levels, whereas light bars represent low water levels. Capital letters denote significance ($p < 0.05$) between high water means whereas lowercase, italicized letters denote significance ($p < 0.05$) between low water means when the main effect was significant ($p < 0.005$).

MUF $g^{-1} h^{-1}$ within the saltgrass plots to 0.359 ± 0.029 nmol MUF $g^{-1} h^{-1}$ within the transition plots, though there was no significant difference between activity within the saltgrass and mangrove plots.

Activity of XY was nearly $3\times$ higher during low water than high water and was significantly different with depth and vegetation community during both seasons (Table 1, Figure 7). Greatest XY activity during high water was within the saltgrass plots, averaging 0.520 ± 0.030 nmol MUF $g^{-1} h^{-1}$, while the lowest activity was within the mangrove and transition plots, which were not significantly different from each other (Figure 4). During low water, XY activity was also highest within the saltgrass plots, followed by the transition plots, and lowest within the mangroves.

Both vegetation community and depth significantly predicted AP activity during both high and low water (Table 1, Figure 8), though activity was nearly $3\times$ higher during the low-water sampling. High-water AP activities averaged 4.52 ± 0.303 nmol MUF $g^{-1} h^{-1}$ within the saltgrass plots, 2.55 ± 0.291 nmol MUF $g^{-1} h^{-1}$ within the transition plots, and 3.05 ± 0.535 nmol MUF $g^{-1} h^{-1}$ within the mangrove plots, though there was no significant difference in activity between the transition and mangrove plots (Figure 4).

Activity of AS was roughly $2\times$ higher during low water than high water, averaging 0.483 ± 0.037 nmol MUF $g^{-1} h^{-1}$ during high water and 0.935 ± 0.100 nmol MUF $g^{-1} h^{-1}$ during low water. Both vegetation community and depth were significant predictors of AS activity in both low water and high water (Table 1, Figure 8). High-water AS activity ranged from 0.572 ± 0.027 nmol MUF $g^{-1} h^{-1}$ within the saltgrass plots to 0.396 ± 0.031 nmol

MUF $g^{-1} h^{-1}$ in the transition plots. Low-water activity was also highest in the saltgrass plots and lowest in the mangrove plots.

Depth predicted NAG activity during both low and high water (Table 1); community type had no effect during either season. N-acetyl- β -D-glucosidase activity was roughly $2.75\times$ higher during the low-water season. All enzyme activity was significantly correlated with each other during both high and low water (Supplementary Table).

Porewater Nutrients

During high water, porewater NH_4 was higher within the mangrove plots (7.15 ± 0.335 mg $NH_4 L^{-1}$) and lowest within the saltgrass and transition plots (2.80 ± 0.776 mg $NH_4 L^{-1}$), which were not significantly different from each other (Table 1). Vegetation community similarly affected porewater NH_4 concentrations during the low-water season, though all concentrations were higher (13.7 ± 0.513 , 7.63 ± 1.12 , and 9.77 ± 1.24 mg $NH_4 L^{-1}$, for the mangrove, transition, and saltgrass, respectively). Depth did not significantly affect porewater NH_4 values during either high or low water.

Vegetation community significantly affected porewater SRP concentrations during both seasons (Table 1), though concentrations were slightly higher during low water. High-water porewater SRP concentrations were greatest in the mangrove plots, averaging 0.460 ± 0.053 mg L^{-1} . The transition zone and saltgrass plot concentrations were not different from each other. During low water, porewater SRP concentrations averaged 0.507 ± 0.068 mg L^{-1} , 0.185 ± 0.061 mg L^{-1} , and 0.402 ± 0.109 mg L^{-1} , within the mangrove, transition, and saltgrass plots, respectively. Similar to pre-

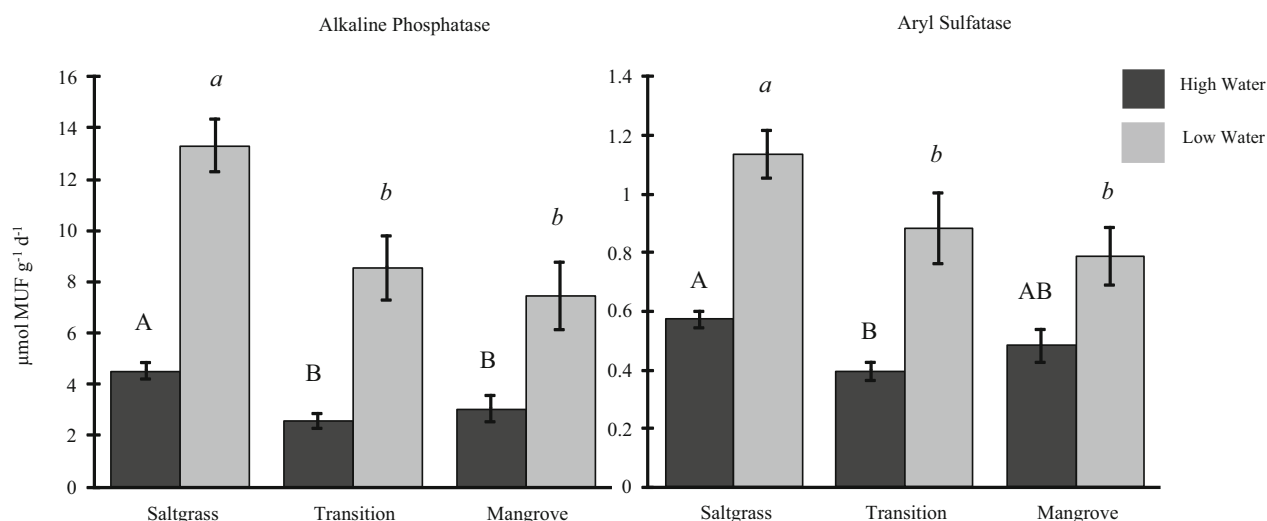


Figure 8. Enzyme activity of extracellular enzymes (AP and AS) at high water and low water along transects of saltgrass, transition, and mangroves. Values are mean \pm standard error ($n = 9$). Dark bars represent high water levels, whereas light bars represent low water levels. Capital letters denote significance ($p < 0.05$) between high water means, whereas lowercase, italicized letters denote significance ($p < 0.05$) between low water means when the main effect was significant ($p < 0.005$).

water ammonium, porewater SRP concentrations did not differ with depth during high water, but were significant during low water (Table 1). Porewater SRP concentrations were relatively stable from the surface to 30 cm and then increased between 30 cm and 35 cm.

Porewater dissolved organic C (DOC) differed between vegetation community types during high water and low water (Table 1). Concentrations of porewater DOC during high water were greatest in the mangrove plots, averaging 11.7 ± 0.670 mg L⁻¹, and lowest in the transition zone, where concentrations averaged 6.87 ± 1.00 mg L⁻¹. The saltgrass plots and transition zone plots were not significantly different from each other during high water or low water. Low-water mangrove porewater DOC concentrations averaged 14.7 ± 0.557 mg L⁻¹, 11.1 ± 1.032 mg L⁻¹, and 11.7 ± 0.777 mg L⁻¹, within the mangrove, transition zone, and saltgrass plots, respectively. Depth also significantly controlled concentrations of DOC in the porewater during the low-water season (Table 1). Values were highest within the top depth interval and then decreased sharply between 0–5 cm and 10–15 cm. Below 15 cm, values increased to roughly half the concentrations in the top depth interval and stayed constant throughout the rest of the depth profile.

DISCUSSION

Carbon Dynamics

One of the prevailing foci of research into mangrove encroachment concerns the effects to soil C stores. In this study, unexpectedly, soil CO₂ production did not differ between vegetation types (Figure 6), coinciding with the null hypothesis (Figure 1, panel A). Studies have hypothesized that the structural differences between mangrove roots and the rhizomes of salt marsh plants will affect oxygenation of the soil, with mangroves hypothesized to exude more oxygen (Scholander and others 1955; Comeaux and others 2012). In a study within a salt marsh in coastal Louisiana, Perry and Mendelsohn (2009) reported higher Eh values in *Avicennia*-dominated plots, compared to *Spartina*-dominated plots. This higher Eh from root exudation of O₂ has been generally believed to enhance soil CO₂ production in soils dominated by mangrove roots, as oxygen provides a terminal electron acceptor thermodynamically favored over sulfate reduction (Perry and Mendelsohn 2009; Comeaux and others 2012; Kelleway and others 2017). Yet, very few studies have documented soil CO₂ efflux from *Avicennia*-dominated soils compared to salt marsh-dominated soils, and they have reported conflicting results (Livesley and Andrusiak 2012; Barreto and others 2018; Simpson and others 2019). In this study, soil CO₂ production was similar throughout vegetation types and salinity and

inundation regimes, leading to the assumption that rate of soil organic matter decomposition is relatively stable across this ecotonal transition (that is, the null hypothesis, Figure 1, panel A). This is surprising not only in relation to oxygen availability, but also when considering differences in microclimate, litter fall, belowground biomass, and other soil physicochemical differences that could occur between sites (Kelleway and others 2017). Though not measured within this study, mangrove cover has been documented to provide shade (Krauss and others 2008), which can lower the temperature of soils beneath mangroves compared to those with herbaceous salt marsh cover. Additionally, mangroves are woody species that contain higher ratios of recalcitrant C compounds, such as lignin, within leaf litter relative to salt marsh grasses, such as saltgrass (Bianchi and others 2013). These recalcitrant C compounds require more energy to be mineralized than labile, low molecular weight compounds, and thus are thought to decompose slower. Other studies have hypothesized that the proliferation of these high molecular weight compounds within mangrove plots might limit decomposition, and subsequently CO₂ production as well, which was not observed in this study. Instead, the similar rates of CO₂ production between vegetation types could reflect unique microbiota between the two vegetation types (that is, Barreto and others 2018), or the interaction of vegetation with present abiotic gradients. Although microbial community composition was not quantified in this study, MBC was similar across the ecotone during high water and weakly correlated with CO₂ production during low water (Figure 6). Finally, CO₂ production rates reported in this study represent potential rates derived from bottle incubations. Although the rates of CO₂ produced during bottle incubations have been shown to closely mimic those found with in situ studies (Breithaupt and others unpublished), repeated in situ measurements would be beneficial in confirming if CO₂ production is indeed unaltered by mangrove encroachment, particularly if one desired to assess the effects of both vegetation and existing abiotic gradients concurrently.

Generally, the mangrove–salt marsh ecotone literature has focused on quantifying changing stocks of C (Kelleway and others 2017 and references therein). Some studies have reported no change in soil C stocks with regards to vegetation (Perry and Mendelsohn 2009; Henry and Twilley 2013; Doughty and others 2016), whereas others have asserted that mangrove soils contain higher concentrations of total C (Osland and others 2012;

Bianchi and others 2013; Lewis and others 2014; Yando and others 2016; Simpson and others 2017), with implications for C sequestration in the face of climate change. This study takes this idea a step further, evaluating carbon dynamics not only in the two end-member communities, but also within the transition zone where both species co-dominate. Surprisingly, our data conflict with previous work, showing not only does the saltgrass contain roughly 65% more soil C than the mangrove plots, but the transition zone generally functions more similarly to the mangrove community, rather than as a true intermediate (supporting hypothesis F in Figure 1). The position of mangrove plots lower in the tidal frame could contribute to export of C in the form of leaf litter through tidal cycles, resulting in lower soil C than the saltgrass plots from the lack of litter being incorporated into the soil matrix (Bouillon and others 2008). Furthermore, following the freeze of 1989, mangroves died back within this region of central Florida, and as a result, the mangrove plots within this field study are not more than 29 years old (Dr. Paul Schmalzer, personal communication). The relatively young age of these trees could account for the small C accumulation rates; with time, mangrove soil C content could surpass that of the saltgrass (Osland and others 2012).

Enzyme activities of BG, XY, and CB also offer some insight into the dynamics of C cycling within this system. The activity of soil extracellular enzymes is correlated with both the availability of substrates and the microbial need for energy sources (Tabatabai 2003). Specifically, BG and CB hydrolyze different forms of cellulose within wetland soils, resulting in either B-D-glucose or cellobiose, respectively (Dunn and others 2014). During high water, both BG and CB expressed greater activity within the end members than in the transition zone (Figures 1C, 7). Under the evolutionary economic hypothesis, enzyme activity is the inverse of availability (Allison and others 2011); for example, high activities of BG and CB within the mangrove and saltgrass plots relative to the transition indicate a depressed availability of cellulose within the end-member soils. Meanwhile, the transition zone has an increased availability of cellulose, likely from either the combined litterfall of mangrove leaves and herbaceous grasses, or through root production. This low activity indicates that greater species richness and evenness in the transition zone alleviate the cellulose limitation. Hemicellulose, a more recalcitrant and less structurally stable form of C (Reddy and DeLaune 2008), is also degraded differentially across the ecotone. Xylosidase is

indicative of the final stage of hydrolysis of hemicellulose into monomers such as xylan (Dunn and others 2014). The high XY activity within the saltgrass plots indicates a high demand (and thus low supply) of hemicellulose, while activities within the transition zone and mangrove plots demonstrate a low demand (and high supply) of hemicellulose (Figures 1F, 7). This is intuitive, as mangroves contain a higher proportion of recalcitrant compounds such as hemicellulose (Bianchi and others 2013), depressing the activity of XY within the mangrove and transition zone soils. Collectively, these C cycling enzymatic activities imply that availability of cellulose for microbial respiration is highest in the transition zone, while availability of hemicellulose is greatest wherever mangroves are present. The presence of mangroves amplifies the availability, likely through increasing the quantity, of cellulose and hemicellulose substrates for microbial respiration within these soils. Except for the same changes in XY, this general trend was only present during high water (Figure 7) and was likely obscured during the low-water season due to exceptionally high rates across the entire site from dry down.

Nitrogen Dynamics

The different vegetation communities and physical characteristics along the transect also altered nitrogen dynamics and speciation. Though extractable NH_4^+ concentrations were highest within the saltgrass and transition zone plots (Figure 5), porewater NH_4^+ concentrations were greatest within the mangrove plots, following the tipping point hypothesis (Figure 1F). Extractable NH_4^+ encompasses both porewater NH_4^+ and NH_4^+ ions adhered to the soil cation exchange complex (CEC) (DeLaune and others 2013). The high availability of porewater NH_4^+ within the mangrove plots could be mediated by salinity: exposure to high salinities can result in the replacement of NH_4^+ on the cation exchange complex with other mono- or divalent ions present in seawater (Steinmuller and Chambers, 2018). Comparatively, NH_4^+ within the saltgrass and transition zone plots, which experience a lower salinity, might still be adhered to the CEC and not released into the porewater. In addition to abiotic forcings such as salinity, available concentrations of NH_4^+ are also mediated by plant uptake (Brannon 1973). Rates of PMN indicate the transition zone and mangrove soils produce less NH_4^+ through the breakdown of organic matter than soils within the saltgrass plots (Figure 5). Extractable NH_4^+ con-

centrations are also affected by oxygen availability within the soils and could thus be explained by more anoxic mangrove soils. Potentially mineralizable N is mediated by available organic matter (which is greatest within the saltgrass plots), quality of organic matter, available NH_4^+ concentrations, and resident microbial communities (Roy and White 2013).

Differences in nitrate availability were observed between high and low water, likely mediated by changes in soil redox potential. As soils dried down during the low-water season, nitrate availability increased as the system became more oxidized, promoting nitrification, the microbially mediated oxidation of NH_4^+ to NO_3^- (Reddy and DeLaune 2008). The drop in water level during the low-water season not only catalyzed changes in speciation of N, but increased the activity of all enzymes, as well as CO_2 production.

Phosphorus and Sulfur Cycling

The abundance of total P within the saltgrass soils compared to the transition and mangrove soils may be related to the high content of organic matter within the saltgrass soils and changes in bulk density across the landscape gradient. When accounting for bulk density (transforming total P into units of density by multiplying by soil bulk density), differences in total P are no longer as apparent. The more tidally influenced mangrove site has a higher bulk density due to less volume for pore space and organic matter, while the saltgrass plots have a higher total P concentration from high organic matter content, effectively evening out the difference between plots. Alkaline phosphatase activity represents this difference in organic versus inorganically bound P present within the vegetation communities (Figure 8). Depressed activity within the transition and mangrove sites indicates that there is plenty of P available for microbial processes, while high activity within the saltgrass site represents increased rates of breakdown of organically bound P monoesters to satisfy microbial needs for P.

Sulfate is one of the most dominant ions within seawater. As the mangrove plots contained the highest salinity, followed by the transition zone plots, it follows that activity of AS would be depressed within these two zones (Figure 8). The availability of sulfate is therefore lowest within the saltgrass plots, owing to their lower salinity, dampened inundation regime, and increased activity of AS. Aryl sulfatase liberates sulfate ions from plant-derived detritus to supply to growing

vegetation. In a previous study at this site, it was observed that saltgrass emitted high rates of various sulfur compounds (H_2S , DMS, CS_2 , and DMDS), and thus concluded that these high rates indicate that saltgrass might utilize sulfonium compounds within their osmoregulatory system (Cooper and others 1986). Utilization of such sulfur-containing ions could promote the liberation of sulfate ions for further uptake by plants.

CONCLUSIONS

The encroachment of mangroves onto into saltgrass in coastal wetlands catalyzes biogeochemical change by altering long-term storage of nutrients and generally affecting indicators of C, N, and P cycling. Of all the hypotheses postulated, the majority of the data collected showed a tipping point in biogeochemical response where the transition zone soils were functionally similar to soils within the mangrove zone. More specifically, longer-term nutrient storage (that is, total soil C, N, P, organic matter content) within the transition zone was functionally equivalent to the mangrove zone (Figure 1F), indicating that encroachment rapidly affects these long-term nutrient storage. Enzyme activity, mineralization rates, and microbial biomass, all indicators of current biogeochemical cycling, appeared to either be more affected by seasonality and environmental variation, rather than encroachment. Based on the total nutrient pool response, it is likely that these short-term indicators will reach a 'tipping point', likely correlated with shifting ratios of mangrove: saltgrass dominance, where biogeochemical processing in the transition zone will function equivalently to the mangrove soils, with implications for macronutrient cycling within this system as a whole.

Though CO_2 production, a proxy for decomposition potential along the ecosystem gradient, did not change with vegetation communities, long-term stores of C (total C, organic matter) were lower within the mangrove zone. As mangrove encroachment continues to occur, this can alter the C balance within the system, potentially affecting the source/sink dynamics of this system. The differences observed within utilization of specific C compounds via measurements of enzyme activity indicate that C breakdown is occurring differently across the ecotone; these effects were not present between both seasons and are relatively short-term indicators of biogeochemical change.

Regarding nutrient availability, seasonal differences affected speciation of N, while the biotic and

abiotic environmental gradients effected PMN rates, porewater NH_4^+ availability, and activity of AP. Encroachment of mangroves, coupled with a higher salinity and water level, increased the amount of bioavailable NH_4^+ within the soils while simultaneously decreasing rates of mineralization of N, though this changes seasonally. Alkaline phosphatase activity indicates the same trend, with decreased AP activity within the mangrove and transition zones indicating higher availability.

Another facet of this study is the linkage between salinity, inundation, and encroachment of mangroves into salt marsh. These results corroborate previous studies suggesting the landward transgression of mangroves is catalyzed by changes in salinity and inundation regimes, as mangroves can occupy a lower place in the tidal frame and withstand high salinities (Egler 1952; Clarke and Hannon 1970; Lugo and Snedaker 1974; Wolanski 1992; Ross and others 2000; McKee and others 2012). Future work is needed to disentangle which biogeochemical parameters are more affected by the biotic change (that is, mangrove encroachment) from those driven by the co-occurring abiotic gradients (that is, salinity and water level).

ACKNOWLEDGEMENTS

The authors would like to thank the entirety of the Aquatic Biogeochemistry Laboratory for their field assistance, especially Dr. Joshua Breithaupt and Nia Hurst for their helpful comments on the manuscript. We would also like to acknowledge Russell Lowers and Dr. Paul Schmalzer for their help in the field and invaluable knowledge of the site.

REFERENCES

- Akaike H. 1974. A new look at the statistical identification model. *IEEE Trans Automat Contr* 19:716.
- Akaike H. 1983. Information measures and model selection. *Int Stat Inst* 44:277–91.
- Allison SD, Weintraub MN, Gartner TB, Waldrop MP. 2011. Evolutionary-economic principles as regulators of soil enzyme production and ecosystem Function. In: Shukla G, Varma A, Eds. *Soil enzymology*. Berlin: Springer. pp 229–43. https://doi.org/10.1007/978-3-642-14225-3_12.
- Andersen JM. 1976. An ignition method for determination of total phosphorus in lake sediments. *Water Res* 10:329–31. [https://doi.org/10.1016/0043-1354\(76\)90175-5](https://doi.org/10.1016/0043-1354(76)90175-5).
- Barreto CR, Morrissey EM, Wykoff DD, Chapman SK. 2018. Co-occurring mangroves and salt marshes differ in microbial community composition. *Wetlands* 38:497–508.
- Bertness MD. 1991. Zonation of *Spartina Patens* and *Spartina Alterniflora* in New England salt marsh. *Ecology* 72:138–48. <https://doi.org/10.2307/1938909>.
- Bianchi TS, Allison MA, Zhao J, Li X, Comeaux RS, Feagin RA, Kulawardhana RW. 2013. Historical reconstruction of man-

- grove expansion in the Gulf of Mexico: Linking climate change with carbon sequestration in coastal wetlands. *Estuar Coast Shelf Sci* 119:7–16. <http://www.sciencedirect.com/science/article/pii/S027277141200457X>. Accessed 30/03/2017.
- Bonferroni CE. 1936. Teoria statistica delle classi e calcolo delle probabilità. Pubblicazioni del R Istituto Superiore di Scienze Economiche e Commerciali di Firenze 8:3–62.
- Bouillon S, Connolly RM, Lee SY. 2008. Organic matter exchange and cycling in mangrove ecosystems: recent insights from stable isotope studies. *J Sea Res* 59:44–58.
- Bozdogan H. 1987. Model selection and akaike's information criterion (AIC): the general theory and its analytical extensions. *Psychometrika* 52:345–70. <https://doi.org/10.1007/BF02294361>.
- Brannon JM. 1973. Seasonal variation of nutrients and physicochemical properties in the salt marsh soils of Barataria Bay, Louisiana.
- Bridgman SD, Ye R. 2013. Organic matter mineralization and decomposition. In: DeLaune RD, Reddy KR, Richardson CJ, Megonigal JP, Eds. *Methods in biogeochemistry of wetlands*, SSSA Book Series 10. Madison, WI: SSSA. pp 385–406. <http://doi.org/10.2136/sssabookser10.c20>.
- Brockmeyer RE, Hinkle CR, Collazo JA, Blum LK, Cahoon DR, Stewart JB, Provancha MJ, Scheidt DM. 2005. Wetlands initiative at Merritt Island national wildlife refuge: project overview, site description and history. *Tech Bull Fla Mosq Control Assoc* 6:14–15.
- Burnham KP, Anderson DR. 2002. *Model selection and multi-model inference: a practical information-theoretic approach*. New York: Ecol Model.
- Cavanaugh KC, Kellner JR, Forde AJ, Gruner DS, Parker JD, Rodriguez W, Feller IC. 2014. Poleward expansion of mangroves is a threshold response to decreased frequency of extreme cold events. *Proc Natl Acad Sci* 111:723 LP-727. <http://www.pnas.org/content/111/2/723.abstract>.
- Clarke LD, Hannon NJ. 1970. The mangrove swamp and salt marsh communities of the Sydney district: III. Plant growth in relation to salinity and waterlogging. *J Ecol* 58:351–69.
- Comeaux RS, Allison MA, Bianchi TS. 2012. Mangrove expansion in the Gulf of Mexico with climate change: implications for wetland health and resistance to rising sea levels. *Estuar Coast Shelf Sci* 96:81–95.
- DeLaune RD, Reddy KR, Richardson CJ, Megonigal JP. 2013. *Methods in biogeochemistry of wetlands*. Madison: Soil Science Society of America.
- Donnelly JP, Bertness MD. 2001. Rapid shoreward encroachment of salt marsh cordgrass in response to accelerated sea-level rise. *Proc Natl Acad Sci U S A* 98:14218–23.
- Doughty CL, Langley JA, Walker WS, Feller IC, Schaub R, Chapman SK. 2016. Mangrove range expansion rapidly increases coastal wetland carbon storage. *Estuaries Coasts* 39:385–96.
- Duarte CM, Losada IJ, Hendriks IE, Mazarrasa I, Marbà N. 2013. The role of coastal plant communities for climate change mitigation and adaptation. *Nat Clim Change* 3:961. <https://doi.org/10.1038/nclimate1970>.
- Dunn OJ. 1961. Multiple comparisons among means. *J Am Stat Assoc* 56:52–64. <https://www.tandfonline.com/doi/abs/10.1080/01621459.1961.10482090>.
- Dunn C, Jones TG, Girard A, Freeman C. 2014. Methodologies for extracellular enzyme assays from wetland soils. *Wetlands* 34:9–17.
- Egler FE. 1952. Southeast saline Everglades vegetation, Florida and its management. *Vegetatio* 3:213–65.
- Feller IC. 1995. Effects of nutrient enrichment on growth and herbivory of dwarf red mangrove (*Rhizophora mangle*). *Ecol Monogr* 65:477–505.
- Feller IC, Whigham DF, O'Neill JP, McKee KL. 1999. Effects of nutrient enrichment on within-stand cycling in a mangrove forest. *Ecology* 80:2193–205.
- Feller IC, Whigham DF, McKee KL, Lovelock CE. 2003. Nitrogen limitation of growth and nutrient dynamics in a disturbed mangrove forest, Indian River Lagoon, Florida. *Oecologia* 134:405–14.
- Feller IC, Chamberlain AH, Piou C, Chapman S, Lovelock CE. 2013. Latitudinal patterns of herbivory in mangrove forests: consequences of nutrient over-enrichment. *Ecosystems* 16:1203–15.
- Field CB, Osborn JG, Hoffman LL, Polsenberg JF, Ackerly DD, Berry JA, Björkman O, Held A, Matson PA, Mooney HA. 1998. Mangrove biodiversity and ecosystem function. *Glob Ecol Biogeogr* 7:3–14.
- Foster TE, Stolen ED, Hall CR, Schaub R, Duncan BW, Hunt DK, Dreese JH. 2017. Modeling vegetation community responses to sea-level rise on Barrier Island systems: a case study on the Cape Canaveral Barrier Island complex, Florida, USA. *PLoS One* 12:1–22. <https://doi.org/10.1371/journal.pone.0182605>.
- Henry KM, Twilley RR. 2013. Soil development in a coastal Louisiana wetland during a climate-induced vegetation shift from salt marsh to mangrove. *J Coast Res* 292:1273–83. <http://www.bioone.org/doi/abs/10.2112/JCOASTRES-D-12-00184.1>.
- Kelleway JJ, Saintilan N, Macreadie PI, Skilbeck CG, Zawadzki A, Ralph PJ. 2016. Seventy years of continuous encroachment substantially increases 'blue carbon' capacity as mangroves replace intertidal salt marshes. *Glob Chang Biol* 22:1097–109.
- Kelleway JJ, Cavanaugh K, Rogers K, Feller IC, Ens E, Doughty C, Saintilan N. 2017. Review of the ecosystem service implications of mangrove encroachment into salt marshes. *Glob Chang Biol* 23:3967–83.
- Kirwan ML, Megonigal JP. 2013. Tidal wetland stability in the face of human impacts and sea-level rise. *Nature* 504:53. <https://doi.org/10.1038/nature12856>.
- Krauss KW, Lovelock CE, McKee KL, López-Hoffman L, Ewe SML, Sousa WP. 2008. Environmental drivers in mangrove establishment and early development: a review. *Aquat Bot* 89:105–27. <http://www.sciencedirect.com/science/article/pii/S0304377008000089>.
- Krauss KW, From AS, Doyle TW, Doyle TJ, Barry MJ. 2011. Sea-level rise and landscape change influence mangrove encroachment onto marsh in the Ten Thousand Islands region of Florida, USA. *J Coast Conserv* 15:629–38.
- Lewis DB, Brown JA, Jimenez KL. 2014. Effects of flooding and warming on soil organic matter mineralization in *Avicennia germinans* mangrove forests and *Juncus roemerianus* salt marshes. *Estuar Coast Shelf Sci* 139:11–19. <https://doi.org/10.1016/j.ecss.2013.12.032>.
- Livesley SJ, Andrusiak SM. 2012. Temperate mangrove and salt marsh sediments are a small methane and nitrous oxide source but important carbon store. *Estuar Coast Shelf Sci* 97:19–27. <http://www.sciencedirect.com/science/article/pii/S0272771411004537>.

- Lugo AE, Snedaker SC. 1974. The ecology of mangroves. *Annu Rev Ecol Syst* 5:39–64. <https://doi.org/10.1146/annurev.es.05.110174.000351>.
- Lunstrum A, Chen L. 2014. Soil carbon stocks and accumulation in young mangrove forests. *Soil Biol Biochem* 75:223–32. <http://www.sciencedirect.com/science/article/pii/S003807171400128X>.
- McKee K, Rogers K, Saintilan N. 2012. Response of Salt Marsh and Mangrove Wetlands to Changes in Atmospheric CO₂, Climate, and Sea Level. In: Middleton BA, Ed. *Global change and the function and distribution of wetlands*. Dordrecht: Springer. pp 63–96. https://doi.org/10.1007/978-94-007-4494-3_2.
- Middleton BA, Mckee KL. 2014. Degradation of mangrove tissues and implications for peat formation in Belizean island forests. *J Ecol* 89:818–28.
- Morris JT, Sundareshwar P V, Nietch CT, Kjerfve B, Cahoon DR. 2002. Responses of coastal wetlands to rising sea level. *Ecology* 83:2869–77. [http://www.esajournals.org/doi/full/10.1890/0012-9658\(2002\)083\[2869:ROCWTR\]2.0.CO;2](http://www.esajournals.org/doi/full/10.1890/0012-9658(2002)083[2869:ROCWTR]2.0.CO;2).
- Osland MJ, Spivak AC, Nestlerode JA, Lessmann JM, Almario AE, Heitmuller PT, Russell MJ, Krauss KW, Alvarez F, Dantin DD, Harvey JE, From AS, Cormier N, Stagg CL. 2012. Ecosystem development after mangrove wetland creation: plant–soil change across a 20-year chronosequence. *Ecosystems* 15:848–66.
- Perry CL, Mendelssohn IA. 2009. Ecosystem effects of expanding populations of *Avicennia germinans* in a Louisiana salt marsh. *Wetlands* 29:396–406. <http://link.springer.com/10.1672/08-100.1>.
- Pontee N. 2013. Defining coastal squeeze: a discussion. *Ocean Coast Manag* 84:204–7. <http://www.sciencedirect.com/science/article/pii/S0964569113001786>.
- Raabe EA, Roy LC, McIvor CC. 2012. Tampa Bay coastal wetlands: nineteenth to twentieth century tidal marsh-to-mangrove conversion. *Estuaries Coasts* 35:1145–62.
- Reddy KR, DeLaune RD. 2008. *Biogeochemistry of wetlands: science and applications*. CRC Press https://books.google.com/books?id=8yLE_tMMTl8C.
- Rogers K, Wilton KM, Saintilan N. 2006. Vegetation change and surface elevation dynamics in estuarine wetlands of southeast Australia. *Estuar Coast Shelf Sci* 66:559–69. <http://www.sciencedirect.com/science/article/pii/S0272771405003562>.
- Ross MS, Meeder JF, Sah JP, Ruiz PL, Telesnicki GJ. 2000. The southeast saline Everglades revisited: 50 years of coastal vegetation change. *J Veg Sci* 11:101–12. <http://www.science.fau.edu/biology/gawliklab/papers/RossMS-et al2000.pdf>.
- Roy ED, White JR. 2013. Measurements of nitrogen mineralization potential in wetland soils. In: *Methods in biogeochemistry of wetlands*. SSSA Book Series SV-10. Madison: Soil Science Society of America. pp 465–71. <http://dx.doi.org/10.2136/sssabookser10.c24>.
- Saintilan N, Wilson NC, Rogers K, Rajkaran A, Krauss KW. 2014. Mangrove expansion and salt marsh decline at mangrove poleward limits. *Glob Chang Biol* 20:147–57.
- Scholander PF, van Dam L, Scholander SI. 1955. Gas exchange in the roots of mangroves. *Am J Bot* 42:92–8.
- Simpson LT, Feller IC, Chapman SK. 2013. Effects of competition and nutrient enrichment on *Avicennia germinans* in the salt marsh-mangrove ecotone. *Aquat Bot* 104:55–9.
- Simpson LT, Osborne TZ, Duckett LJ, Feller IC. 2017. Carbon storages along a climate induced coastal wetland gradient. *Wetlands* 37:1–13.
- Simpson LT, Osborne TZ, Feller IC. 2019. Wetland soil CO₂ efflux along a latitudinal gradient of spatial and temporal complexity. *Estuaries Coasts* 42:45–54. <https://doi.org/10.1007/s12237-018-0442-3>.
- Steinmuller HE, Chambers LG. 2018. Can saltwater intrusion accelerate nutrient export from freshwater wetland soils? an experimental approach. *Soil Sci Soc Am J* 82:283–92. <https://doi.org/10.2136/sssaj2017.05.0162>.
- Tabatabai MA. 2003. Soil enzymes. In: *Encyclopedia of agrochemicals*. American Cancer Society <https://onlinelibrary.wiley.com/doi/abs/10.1002/047126363X.agr354>.
- Torio DD, Chmura GL. 2013. Assessing coastal squeeze of tidal wetlands. *J Coast Res* 29:1049–61.
- Wolanski E. 1992. Hydrodynamics of mangrove swamps and their coastal waters. *Hydrobiologia* 247:141–61.
- Yando ES, Osland MJ, Willis JM, Day RH, Krauss KW, Hester MW, McCulley R. 2016. Salt marsh-mangrove ecotones: using structural gradients to investigate the effects of woody plant encroachment on plant-soil interactions and ecosystem carbon pools. *J Ecol* 104:1020–31.